The basic photoelectron spectroscopic technique involves ionization of the sample atom or molecule M by a beam of monoenergetic photons, in which process, the former loses an electron:

$$M + h\nu \longrightarrow M^+(E_{int}) + e$$

M^+ is the resulting ion formed in the state with internal energy E_{int}, and e is the product photoelectron. E_{int} includes electronic, vibrational and rotational energy of the ions; $E_{int} = 0$ means that the ion is formed in its ground state. In order that photoionization may occur, it is essential that the photon possesses an energy higher than the lowest ionization potential I_p of the sample atom or molecule. It follows that the excess energy available after ionization, $h\nu - I_p - E_{int}$, must appear as translational energy of the products, i.e., the ion and the electron, (Fig. 1.1).

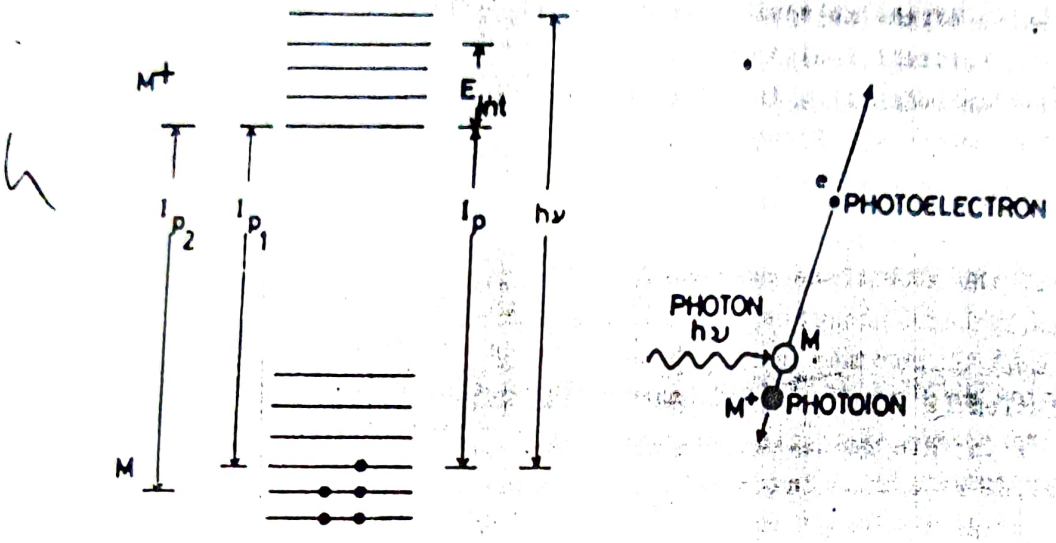

Fig. 1.1 The basic photoionization processes.

Conservation of linear momentum requires that the excess energy be partitioned in inverse proportion to the masses of the products which means that the electron, which is about two thousand times lighter than the lightest atom, secures practically all the excess energy. The error involved in assuming that absolutely all the excess energy appears as the translational energy of the electrons, in the worst case, is of the order of 1 part in 10^4, which is clearly negligible for ordinary applications. For ionization of heavier atoms and molecules, this error is still less. Thus if monoenergetic photons are used for ionization and the photon energy $h\nu$ is known, a simple determination of the kinetic energy of the photoelectrons, which is equal to $h\nu - (I_p + E_{int})$, directly provides the ionization potential of the sample to form its own ion in a certain internal energy state. In the lowest internal energy state of the ion $E_{int} = 0$ and the photoelectrons correspond to the lowest ionization potential of the target particle. Since ionization potentials are characteristic properties of atoms and molecules, the method therefore provides a direct means for chemical analysis. The basic experimental requirements are simple, that of a monoenergetic photon source and an electron energy analyzer.

But not only can the ionising photon remove the most loosely bound electron, if the photon energy is sufficiently high, it can cause removal of other electrons which are tightly bound. With energetic photons thus different electrons are removed, one at a time, and corresponding photoelectrons with energies $h\nu - I_{p1}$, $h\nu - I_{p2}$ etc. are ejected. A photoelectron kinetic energy analysis of such a situation yields a series of ionization potentials I_{p1}, I_{p2}, etc. Since the ionization potential of an electron from a given state is also a close measure of the binding energy of the electron in that state, these two terms sometimes may be used synonymously. It is to be mentioned here that the energy required to populate the ground vibrational state of the molecular ion is called the adiabatic ionization potential. The vertical ionization potential, which is higher than the adiabatic ionization potential, involves ionization to higher vibrational states of the ion and the transition probability of this process, like those in ordinary electronic transitions, is determined by Franck-Condon principle.

The depth to which the atomic and molecular levels can be probed with this technique clearly depends on the upper limit of the photon energy used. Till today, the most common low energy photon sources use helium with HeI resonance radiation ($2^1P \rightarrow 1^1S$) of wavelength 58.4 nm which has an energy of 21.2 eV. With this radiation source, energy states having binding energies upto 21.22 eV can be investigated. Use of resonance radiation from some other species leads to somewhat higher energies (HeII 40.8 eV, $n = 2 \rightarrow 1$). But if orders of magnitude increase in photon energy is sought then one has to resort to x-ray sources like Al K_α (1487 eV), Mg K_α (1254 eV), with energies in keVs. With the availability of high energy photon sources one can thus measure the binding energies of those orbital electrons which are close to the nucleus, i.e., the core electrons. In general, for measurement of binding energies of valence electrons, ultraviolet radiation sources like that from HeI are used, and for core electrons, x-ray sources are used. Although a uniform convention on nomenclatures has yet to emerge, analysis using low energy photon sources has been simply called photoelectron spectroscopy or UV-PES and, when x-ray sources are employed, the term ESCA, Electron Spectroscopy for Chemical Analysis, or XPES is used. The basic physical process involved in both the techniques, however, is the same. The terms PESOS, photoelectron spectroscopy for outer shells, and PESIS, photoelectron spectroscopy for inner shells have also been used for UV-PES and X-PES respectively. The trend, however, is to use the terms UPS and XPS respectively for ultraviolet and x-ray photoelectron spectroscopy. The ranges of some photon sources in relation to molecular nitrogen core and valence orbitals are shown in Fig. 1.2.

At this point it should be mentioned that two other processes may occur simultaneously with photoionization, which can also be used to derive information of the type available from photoelectron spectroscopy. Both

which nomenclatures are made in Auger transitions. The level initially ionized is written first (A), followed by the level from which the electron relaxes (B), and finally the level from which the Auger electron is lost (C). Thus in Fig. 1.4 the transition shown is to be labelled $KL_1L_{2,3}$. In solids, electrons may originate in the valence band. Then KL_1V or KVV may represent suitable Auger transitions. The scheme of Fig. 1.4 is strictly valid for isolated atoms with discrete energy levels. It may be added here that in solids, large valence band populations lead to intense Auger electron intensities. At low primary energies the probability of the x-ray fluorescence efficiency is of the order of 0.05 and the Auger process dominates. Only at transition energies greater than 10 keV, rates of radiative transitions become comparable to Auger transitions.

Returning to photoelectron spectroscopy, let us now look into the nature of information one can obtain on free atoms and molecules, i.e. those in the gaseous state. It is clear that since in the gaseous state perturbations due to neighbouring sample atoms and molecules are negligible, width of the energy levels will solely be their natural width determined by the lifetime. Whether all the energy levels will be actually observed through electron energy analysis depends on the line width of the monochromatic radiation and the resolution of the electron energy analyzer employed.

Experimentally, a photoelectron spectrum is obtained by radiating a beam of photons on the sample, and energy analysing the ejected photoelectrons. After the electron energy analysis, the photoelectron spectrum shows a number of types of photoelectrons which differ in kinetic energy and also in flux. In order to convert this into binding energy information, knowledge of the initial photon energy is necessary, since the photoelectron energy is the difference between the incident photon energy and the binding energy. Thus, with a given sample, depending on the photon source employed, the numerical values in the abscissa scale of the electron intensity-electron kinetic energy plot may be different, but they all reduce to identical binding energy spectrum once information about the incident photon energy is introduced.

Fig. 1.5 shows the photoelectron spectrum of Argon with clearly resolved spin-orbit coupled states $^2P_{3/2}$ and $^2P_{1/2}$. This spectrum was obtained using HeI 21.22 eV radiation. The upper scale on the abscissa represents the kinetic energy of the photoelectrons and the lower scale represents the binding energy, obtained by subtracting the photoelectron kinetic energies from 21.22 eV.

The basic principles which apply to atomic photoelectron spectra are also applicable to photoelectron spectra of molecules. This is illustrated by using the N_2 and N_2^+ energy states. A few low lying potential energy curves of nitrogen are shown in Fig. [illegible]. energy, it can be seen that levels upto the [illegible] can be populated. The population distribution in the various ionic states

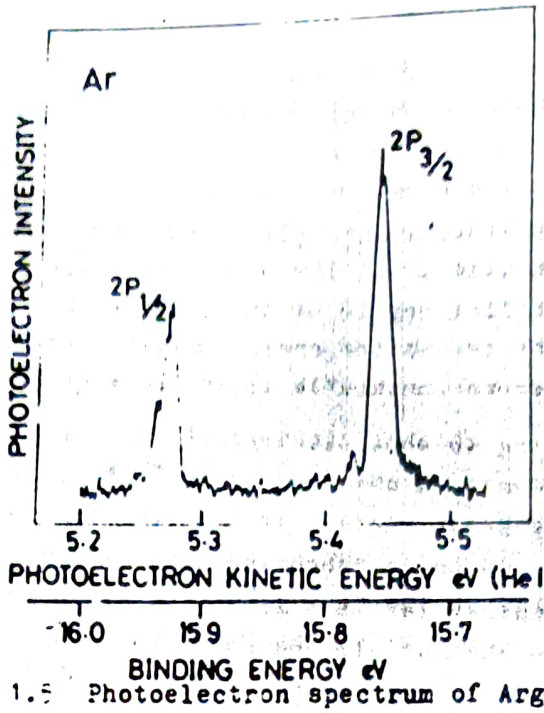

Fig. 1.5 Photoelectron spectrum of Argon.
(7)

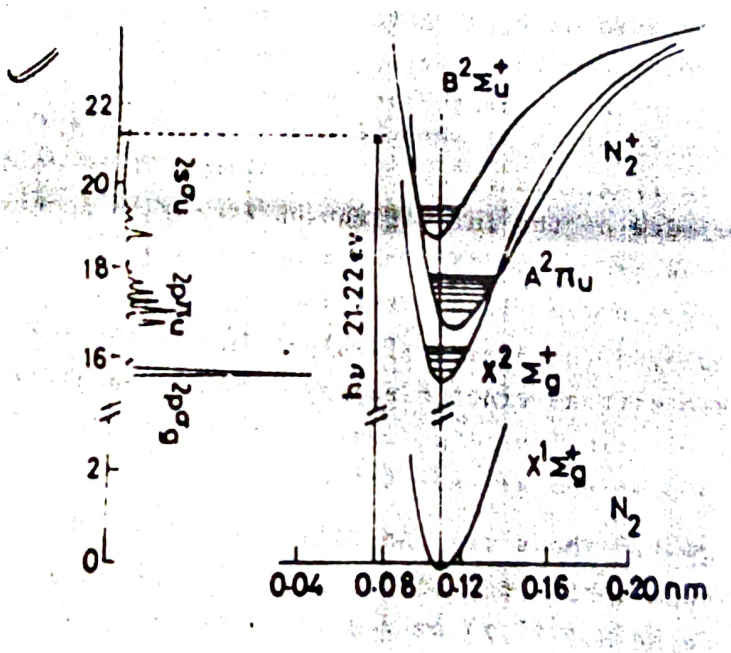

Fig. 1.6 Photoelectron spectrum of N_2.(15)

however depends on the photoionization cross sections to these states at 21.22 eV energy. The fine structure of distribution into vibrational levels of the various electronic states of the ion ordinarily depends on the equilibrium internuclear distances of the electronic states and hence the respective Franck-Condon factors. It will be noticed from Figs. 1.2 and 1.5 that HeI photon energy is only adequate for ionizing upto $\sigma_u 2s$ electrons (to the state $B^2\Sigma_u^+$); the higher binding energy state $\sigma_g 2s$, lying closer to the core, will remain unaffected.

The relative location of the molecular and ionic potential energy curves, which determine the Franck-Condon factors, depends on the nature of the electron orbital from which the electron is lost i.e. whether it is

bonding, antibonding, or nonbonding. This effect, depending on the nature of the orbital involved, causes changes in the vibrational frequency of the ionic states and hence the spacing of the vibrational energy levels. For example, loss of a bonding electron in ionization reduces the charge distribution between the nuclei and hence decreases the force constant of the molecule. Since the vibrational frequency and the force constant k are related by a formula of the type $\nu = (1/2\pi)\sqrt{(k/\mu)}$ where μ is the reduced mass, the effect of decreasing the force constant is also to lower the energy spacing between the vibrational levels. The effect of loss of an antibonding electron is just the opposite. Loss of an antibonding electron strengthens the bond, decreases the internuclear distance, increases the force constant and hence increases the energy spacing between the levels. Nonbonding electron removal has little effect on the internuclear distance and the force constant, and hence the spacing between the vibrational energy levels remains unaffected. This criterion of change in vibrational spacing can be applied to find out whether the molecular orbital involved in ionization has bonding, nonbonding or antibonding characteristics. For example, according to this analysis, the $2p\sigma_g$ orbital is nonbonding (weakly bonding) because the vibrational spacing decreases on ionization from 2345 cm^{-1} (vibrational spacing of the ground state of N_2) to 2191 cm^{-1}, the $2p\pi_u$ is strongly bonding as in the band assigned to it the vibrational spacing decreases drastically from 2345 cm^{-1} to 1850 cm^{-1}, and the $2s\sigma_u$ orbital is essentially nonbonding (weakly antibonding) as the vibrational spacing due to this band increases from 2345 cm^{-1} to 2397 cm^{-1}. While knowledge of the nature of the orbital can be used to predict shifts in vibrational frequencies in spectra, actually a more important application is the reverse study of the changes in vibrational energy level spacings to derive information on the nature of the orbital involved in ionization.

In addition to obtaining the bonding nature of orbitals involved in ionization, vibrational structure in photoelectron spectroscopy is a valuable tool in determination of vibrational energy levels of those molecular ions where absorption or emission spectroscopic work has proved to be very difficult. An example is that of the molecular ion H_2^+ or HBr^+. In many such cases there has been only scant emission spectroscopic work with the help of which vibrational energy level spacings of molecular ions can be obtained, and the question of absorption spectroscopy almost does not arise, as only a handful of gaseous molecular ions have been so far observed in absorption, and that too under rather special experimental conditions. Photoelectron spectroscopy, however, easily gives the energy spectrum of the molecular ionic vibrational levels, and in many cases constitutes a powerful alternative to absorption spectroscopy of gaseous ions. The HeI UPS of HBr^+ is presented in Fig. 1.7 which shows a vibrational progression upto $v' = 6$, wherefrom the vibrational frequencies and the vibrational constants of the ionic state can be easily derived.

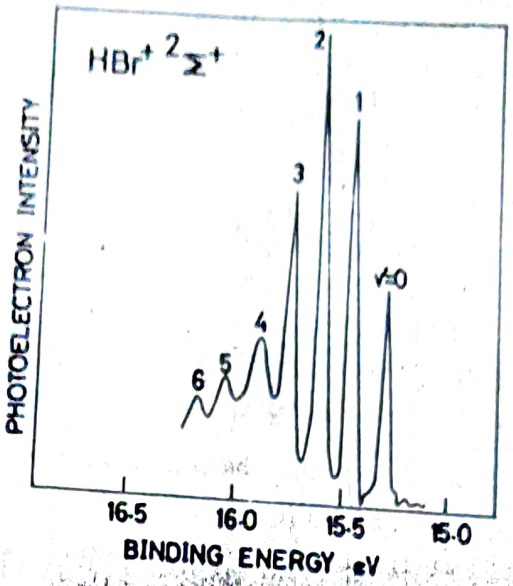

Fig. 1.7. Photoelectron spectrum of HBr. (56)

The scope of application of photoelectron spectroscopy goes far beyond the determination of valence energy levels as pointed out above. Although binding energies of valence electrons can be found out through UPS, several types of additional information can be obtained by using higher energy photons. The major difference between the use of low energy photons and x-rays is that the latter is able to reach the core electrons and ionize them. One of the first applications of XPS is the determination of binding energies of core electrons in various atoms. Since the magnitude of the core electron binding energy is expected to strongly reflect the attractive forces of the nucleus on the core electrons, this should depend on the charge of the nucleus, i.e., the atom chosen, and this makes the core binding energy a characteristic property of the atom considered. It is because of this reason, it finds application in chemical analysis, and out of this originates the acronym ESCA, mentioned earlier. Core binding energies of 1s electrons of the second period elements Li, Be, B, C, N, O and F derived from XPS are shown in Fig. 1.8. The ordinate represents photoelectron count rate which is equivalent to photoelectron intensity. Since the attractive force of the nucleus on the 1s electrons increases with the atomic number, it is natural to expect that the 1s binding energy for these atoms will be the least for lithium and the highest for fluorine. This is found to be correct (1s binding energy for Li = 55 eV, Be = 111 eV, C = 284 eV, N = 399 eV, O = 532 eV and F = 686 eV), and shows, clearly, that photoelectrons from XPS can be used for chemical identification of samples. Intensities of electron peaks from various elements as can be seen in Fig. 1.8 are different, the reason being, that even at a photon energy adequate for ionisation, the ionization cross sections are different for different species. In fact, from a knowledge of such experimental peak intensities, the magnitude of incident photon flux and sample density, it is possible to determine absolute values of photoionization cross sections.

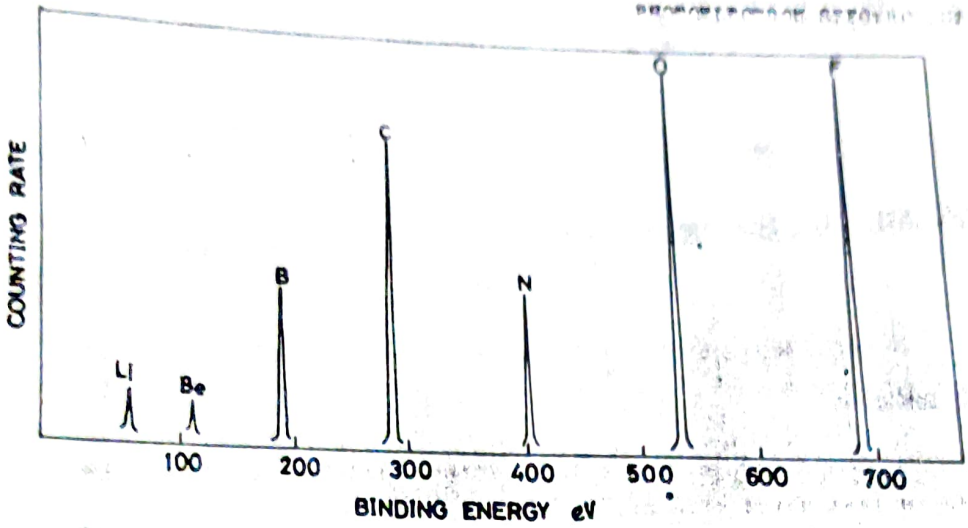

Fig. 1.8 Core (1s) binding energies for second period elements.(1) (solid sample)

Applications of the characteristic core binding energies, however, extend much further. Whereas the binding energy of a certain type of core electron is quite characteristic of a given atom, if XPS is taken of a molecule in which an atom of a particular kind is present, the core photoelectron peak of the atom does not always appear at the same characteristic energy; there is a slight shift depending on the molecule chosen. This happens, because, although the core electron binding energy is principally determined by the nuclear charge, there is some subsidiary effect due to the valence electrons influencing it. More pronounced the effect is of the valence electrons, greater is the expected shift in the binding energy. Since the valence electron distribution would vary depending on the nature of bonding, it is reasonable to expect that the core binding energy would reflect, through chemical shifts, changes in valence charge distributions of the molecule. This is observed in practice, and it is for this reason, the chemical shift of core electron binding energies holds great potential for use as a probe in investigating the nature of bonding in molecules. A simple case of this chemical shift in core binding energy can be seen in the example of carbon monoxide and carbon dioxide. Oxygen atom being more electronegative than carbon we expect that the carbon valence electrons in carbon monoxide will be somewhat shifted towards the oxygen atom. Since this will cause the influence of carbon nucleus on the C 1s electron to increase, its effect will be to make the C 1s electron more strongly bound to the carbon nucleus and hence an increased C 1s core binding energy should result. In carbon dioxide, the presence of two oxygen atoms ought to augment this effect, and the core binding energy should be even higher. This is indeed what is experimentally observed. Carbon 1s core binding energy is found to be 296 eV in carbon monoxide and 297.5 eV in carbon dioxide as compared to 288 eV for the free atom case. In oxygen atom the effect is just the reverse. Availability of the carbon electron should decrease the oxygen 1s binding energy in carbon

monoxide, but the same effect will be somewhat less in carbon dioxide as there is less shift of bonding electrons. Thus the core binding energy for oxygen 1s will be less in carbon monoxide than in carbon dioxide.

Application of these chemical shift principles to larger molecules reinforces this point and demonstrates its scope of applications. Taking the case of ethyl chloroformate, $ClCO.OCH_2CH_3$, one observes that there are three carbon atoms, one in the carbonyl group, one in its somewhat adjacent methylene group, and the third one in the farthest methyl group. All these carbon 1s peaks must be close to 288 eV, the core binding energy of carbon 1s in the free atom, but one should also expect some appropriate chemical shifts depending on the peculiar electronic environment of each of the carbon atoms. The carbonyl carbon, because of its proximity to oxygen must have the highest binding energy as explained earlier, the methylene carbon somewhat lower, and the methyl carbon C 1s the least binding energy. The spectrum of ethyl chloroformate is shown in Fig. 1.9 and the binding

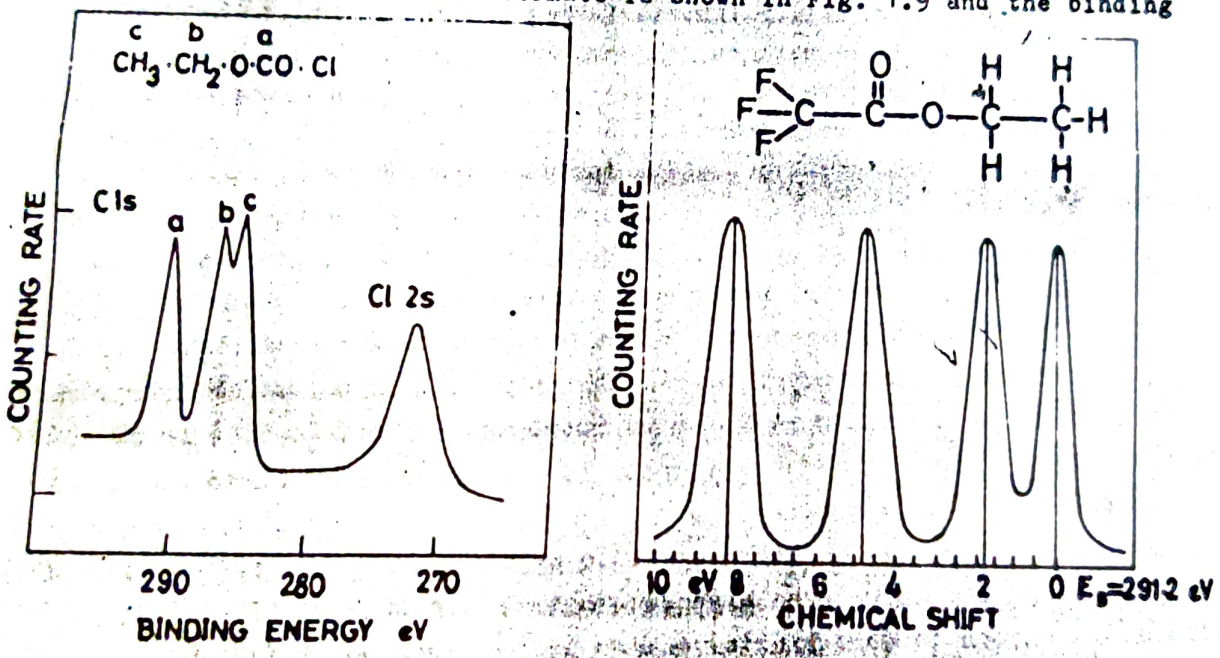

Fig. 1.9 C 1s chemical shifts in ethyl chloroformate and ethyl trifluoroacetate.(15,283)

energies of carbon 1s peaks confirms this analysis. This also shows how it may provide an entirely new technique in organic and in inorganic chemistry for determination of charge distribution, and hence constitute a useful method in structural investigations. The spectrum of ethyl trifluoroacetate, taken at much higher resolution, is also shown in Fig. 1.9 in which the chemically shifted peaks manifest much more clearly. The chemical shifts of the peaks are shown with respect to the C 1s binding energy of CH_3 carbon, which has a binding energy of 291.2 eV. The trifluoromethyl carbon C 1s, with three highly electronegative fluorine atoms, has the highest binding energy.

The process of photoionization described earlier may become quite complicated due to various additional factors, for example, due to occurrence of autoionization. In autoionization, as shown schematically

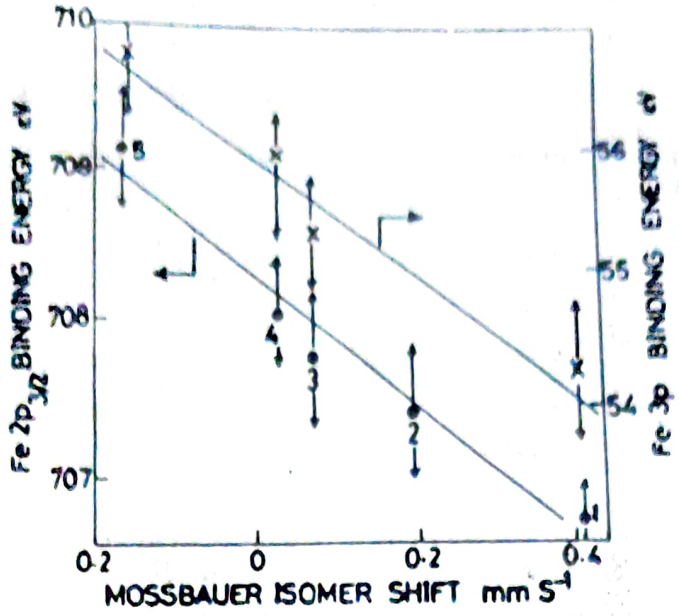

Fig. 3.11 Correlations of Mossbauer shifts with Fe $2p_{3/2}$ and Fe 3p XPS Shifts. (1) $[Fe^{II}(phen)_3][ClO_4]_2$, (2) trans-$Fe(isocy)_4Cl_2$, (3) trans-$Fe(isocy)_4(SnCl_3)_2$, (4) $[Fe(SnCl_3)(isocy)_5][ClO_4]$, and (5) $Na_2Fe(CN)_5NO.2H_2O$. (phen = 1, 10 phenanthroline, isocy = p-methoxy phenyl isocyanide). (132)

XPS-Mossbauer shift correlation of some Fe(II) low spin complexes. $\Delta\langle r^2\rangle$ is negative for the Fe^{57} (14.4 keV) transition. The negative slope of the lines in Fig. 3.11 implies a concurrent decrease of ΔE and $\delta\Delta r^2$ with increase in Mossbauer shift. This corresponds to the case on tne last row in Table 3.10 where both ΔE and $\delta\Delta r^2$ are negative and which indicates a gradual increase in electron population on the iron atom, contributed primarily by increased π-backbonding from the ligands. The Mossbauer isomer shifts are more amenable to interpretation in terms of ground state electron distribution, on the basis of which linear $\delta_A - \Delta E_A$ correlation in a series of compounds should be predictable. It is reasonable to expect that comparisons with XPS shifts would be more meaningful with more dependable information available on nuclear size factors.

Chemical shifts have been effectively employed in elucidation of structure of complex compounds, and we present here one example on biguanide $H_2NC(=NH)NHC(=NH)NH_2$ complexes. There has been a controversy on certain aspects of the structure of biguanide complexes, the ligand forming two types of complexes, (i) in which the uncharged ligand LH forms complexes of the type $[M(LH)_m]^{n+}$, m = 2 or 3, and (ii) in which the deprotonated ligand L^- forms complexes $[M(L)_m]$. Older views speculated the presence of a quarternary nitrogen atom, but recent NMR data indicate its absence in bis (biguanide) nickel II chloride. Ultraviolet absorption studies support formulation of the following structures for the neutral and charged species, involving π electron delocalisation.

Some of the N 1s binding energies of metal biguanides are shown in Table 3.11. The respective line widths (FWHM) are also shown, which happen to be considerably larger than N 1s widths found in compounds containing a single type of nitrogen atoms, these widths being about 1.9 eV. The rather large line widths in the complexes may be taken to indicate a composite spectral structure, due to chemically shifted peaks of different types of nitrogen atoms. For chromium trisbiguanide, a best fit through a Gaussian model is obtained if two 1.9 eV peaks are taken separated by 1.5 eV with relative intensities of 2:3. Table 3.11 also shows that the N 1s binding energy in amines, nitriles and pyridine is in the 398-398.5 eV range and is considerably less than those of simple ammonium salts where the values are above 401 eV. Actually, one might calculate the expected line width assuming that a quarternary atom is present. Using a conservative low value of 1.6 eV for the chemical shift between $-NH_3^+$ and $-NH_2$, a separation of 1.5 eV as observed in the spectrum of chromium trisbiguanide, and expected relative intensities of three types of nitrogen atoms as 1:2:2, a computer simulation predicts a N 1s FWHM linewidth of 3.8 eV, if a quarternary nitrogen atom is present. This is much higher than any one of the widths observed in experimental spectra and this result may be used to rule out the presence of any quarternary nitrogen atom. Further, if π delocalisation does not extend to the N atoms outside the chelate region, differences in N 1s binding energy may be expected for the two types of amino nitrogen atoms. That delocalization actually extends to all the nitrogen atoms is indicated by N 1s binding energies of biguanidine sulphate and guanidinium chloride, and salts of biguanide complexes are thus quite well represented by the structure II.

A somewhat different aspect of core electron spectra has to do with occurrence of satellite lines which are observable in high resolution around the main core electron line, as shown in Fig. 3.12. A few high energy lines that appear in the neon spectrum are due to energy inhomogeneity of the incident x-rays having components of higher energy photons. Some of the lower energy satellite lines are pressure dependent. These arise due to collisions between ejected photoelectrons and neutral atoms, and consequent excitations of the latter with equivalent energy loss of the photoelectrons. The lines which are pressure independent have their origin in the ionization process itself. These satellite lines are due to valence electron excitation, concurrent with the ejection of photoelectrons;

Table 3.1: N 1s Binding Energies for Metal Biguanide Complexes and Related Nitrogen Compounds (133)

Compound		Nitrogen 1s Binding Energy eV	FWHM eV
Biguanide complexes			
$[Cr(C_2N_5H_7)_3]Cl_3$		399.4	2.8
$[Cr(C_2N_5H_6)_3]H_2O$		399.2	3.0
$[Ag(III)(C_2N_5H_7)_2]_2(SO_4)_3$		400.0	2.4
$Cu(C_2N_5H_6\text{-}p\text{-}C_6H_4SO_3)_2$		400.0	2.7
$[Co(C_2N_5H_7)_3]Cl_3$		399.2	2.7
$[Co(C_2N_5H_6)_3]H_2O$		398.9	2.9
$Ni(C_2N_5H_6\text{-}p\text{-}C_6H_4SO_3)_2$		400.2	2.7
$[Ni(C_2N_5H_6)_2]H_2O$		398.9	2.7
$[Cu(C_2N_5H_6)_2]H_2O$		399.5	2.9
$[Cu(C_2N_5H_7)_2]Cl_2$		399.5	2.5
Other nitrogen compounds			
$C_4H_9NH_2$		398.1	-
$(n\text{-}C_4H_9)_3N$		398.1	-
C_6H_4N		398.0	-
C_6H_5CN		398.4	-
$(CH_3)_4N^+Cl^-$		401.5	-
$(NH_4)_2SO_4$		401.5	2.0
NH_4Cl		401.0	1.0
NH_4NO_3	NO_3^-	405.7	1.8
	NH_4^+	402.0	1.8

the lines are thus called the shake-up lines. Depending on the extent to which the valence electrons are excited, the photoelectrons are ejected with that much less energy; hence, the kinetic energy spectrum of the photoelectrons have peaks at correspondingly lower energies from the main photoelectron line. An extreme situation of this shake-up process is the complete loss of a valence electron by ionization, and this process is called the shake-off process. Since this loss of the valence electron generates a doubly charged ion in the ionisation continuum, the photoelectron spectrum shows a broad continuous band due to the shake-off process.

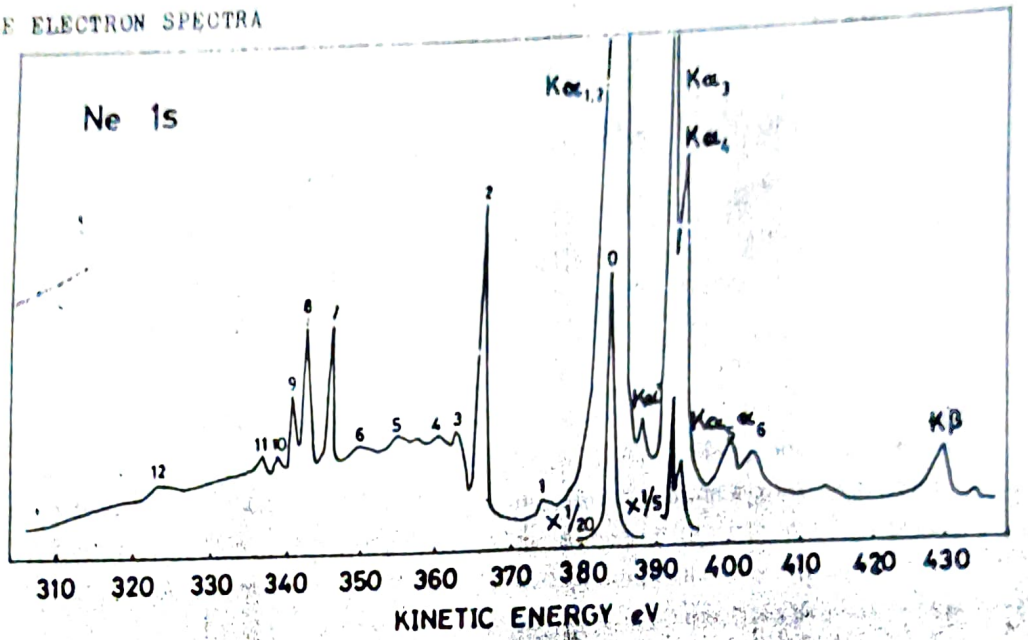

Fig. 3.12 Satellite lines in Ne 1s high resolution core electron spectrum. (4,19,20)

In the Ne 1s high resolution spectrum shown in Fig. 3.12, the line 0 is the main photoelectron line, 1, 5, 6 are satellite lines due to other x-ray lines beside Mg K_α, lines 2, 3, 4 are pressure dependent lines and arise due to collisions with neutral atoms. The line 1 is a satellite of the line 2, and the lines 5, 6 are satellites to the line 7 and the lines 8 + 9. The lines 7, 8, 9, 10, 11, and 12 are due to the shake-up process with transitions shown in Table 3.12 and also schematically in Fig. 3.13.

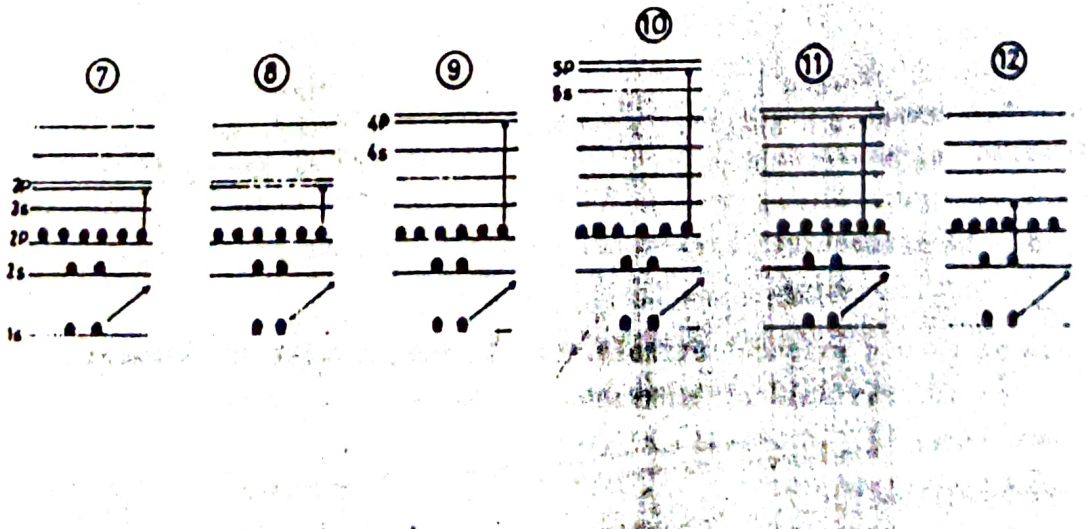

Fig. 3.13 Schematic description of Ne 1s shake-up processes. (4)

In high resolution core electron spectra, the electron shake-up lines are always present, for atoms as well as molecules. Correlation of the shake-up lines with the actual processes and the transitions involved requires accurate knowledge of the energy levels of the ion. Since ... shake-up and shake-off are relaxation processes, a study of shake-up and

... satellites which on the low kinetic energy side of Ne 1s (4)

Line	Relative Energy (eV) with Respect to the Main Peak	Process	Interpretation
	0	Single hole ionization	Ne 1s($Mg K\alpha_{1,2}$)
1	-7.8	$K\alpha_{3,4}$ satellite	to 2
2	-16.8	Energy loss	2p 3s
3	-20.0	Energy loss	2p 3d,4s
4	-22.0	Energy loss	2p ns,nd
5	-28.0	$K\alpha_{3,4}$ satellite	to 7
6	-33.0	$K\alpha_{3,4}$ satellite	to 8 + 9
7	-37.3	Shake-up	2p $3p^2S$
8	-40.7	Shake-up	2p $3p^2S$
9	-42.3	Shake-up	2p $4p^2S$
10	-44.2	Shake-up	2p $5p^2S$
11	-46.4	Shake-up	2p $4p^2S$
12	-60.0	Shake-up	2s $3s^2S$

shake-off spectra can lead to detailed information about relaxation phenomena in atoms and molecules. Many elaborate analysis of shake-up states of atoms have been made. For molecules also, similar studies have been undertaken; Fig. 3.14 shows the shake-up lines associated with N 1s and O 1s in the photoelectron spectra of N_2O.

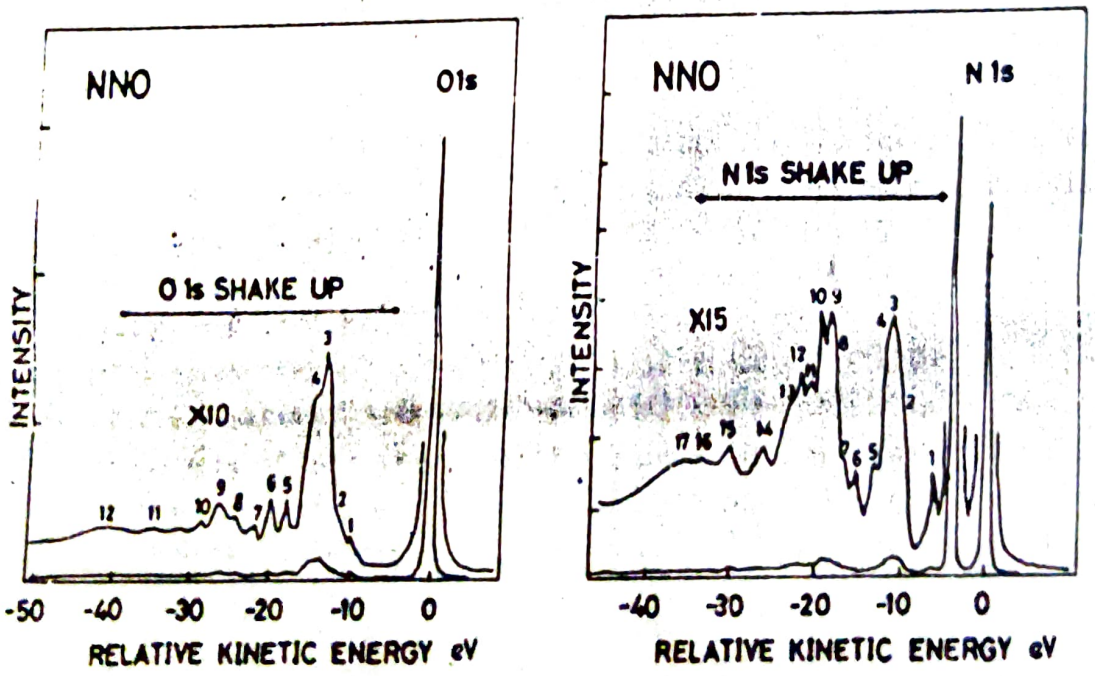

Fig. 3.14 N 1s and O 1s shake-up lines in the core electron spectra of nitrous oxide. (19,20)

The widths of core electron spectral lines provide additional information on processes taking place during photoionization. The lifetime of excited states are determined by probabilities of several types of